

## NUMERICAL ANALYSIS ON THE COLLAPSE OF A RC FRAME

**George Bogdan NICA** –Technical University of Civil Engineering, e-mail: george.nica@utcb.ro

**Florin PAVEL** - Technical University of Civil Engineering, e-mail: florin.pavel@utcb.ro

**Abstract:** This paper focuses on the collapse analysis of a planar RC frame. This research is based on an experimental study presented in the literature. The analyses are conducted using a dedicated software based on the Applied Element Method. This numerical method is able to model accurately all the structural behaviour stages leading up to the collapse itself. A very good match between the experimental and numerical results is observed. The numerical investigation highlights several behaviour stages for the model RC frame. Moreover, the contribution of the RC slab and the impact of the concrete strength on the overall collapse mechanism is discussed and evaluated through numerical investigation.

**Keywords:** Applied element method, failure mechanism, column, slab, displacement.

### 1. Introduction

The progressive collapse of structures is a particularly important research topic, especially in the light of some recent catastrophes, such as the collapse of the Alfred P. Murrah Federal Building in Oklahoma-City in 1995, the collapse of the World Trade Center in 2001, the collapse of the Windsor Tower in Madrid in 2005 or the failure of the Rana Plaza in Bangladesh in 2013 and which has claimed the lives of more than 1000 people. Thus, these type of structural failures can cause, besides the economic damage, large number of casualties. The loads which are responsible for these type of failures can be due to earthquakes, fires, explosions, terrorist attacks, to name just a few possible sources.

In this paper, we analyse the collapse of an experimental RC frame [1] through the use of numerical methods. Specifically, in this paper the Extreme Loading for Structures software [2] which is based on the Applied Element Method is employed for numerical simulations.

The Applied Element Method (AEM) [3] is a quite recent numerical analysis method in which the structure is made up of distinct elements connected by springs. Thus, the discrete cracking of elements which can appear due to large loads of accidental nature is captured accurately.

The experimental RC frame analysed in this paper has been previously analysed by other researchers, as well [4, 5, 6]. In the paper on Botez et al. [4], the experimental RC frame is checked using the Finite Element Method (FEM) and a dedicated software (Abaqus). The authors checked the vertical and horizontal displacements and the vertical reaction and the results showed a good match between the experimental and numerical model for the analysed parameters. Salem et al. [5] employ also the Applied Element Method dedicated software Extreme Loading for Structures and compare numerical and experimental results for the same test RC frame. Their results (failed column axial load versus vertical displacement) are also close to the experimental ones. Li et al. [6] apply the Finite Element Method code MSC.MARC and found a good match between experimental and numerical results.

Additional works on this subject can be found in the papers of Shan et al. [7] in which the influence of infill walls on the progressive collapse of a RC frame is tested. The results shown in Shan et al. [7] reveal that the infill walls can affect to a great extent the performance of RC frames and their failure modes. Fragility functions for low-rise RC frames have been proposed

by Brunesi et al. [8] in order to be implemented in progressive collapse risk analysis. The progressive collapse of the Alfred P. Murrah Federal Building in Oklahoma-City is studied in the paper of Kazemi-Moghaddam and Sasani [9]. The authors conclude after performing their analyses that the initial damage suffered by the building must have been more severe than the sudden loss of a column. The progressive collapse (both experimental and numerical) of a flat plate RC structure is studied by Kokot et al. [10]. The design methods available in various guides or codes which could be used in order to resist progressive collapse are presented by Wang et al. [11]. The collapse of the Minnesota I-35W bridge and its causes are evaluated through the use of the Applied Element Method by Salem and Helmy [12].

In this paper, we extend the previously mentioned analyses and focus in more detail on the collapse mechanism of the experimental planar RC frame [1]. Consequently, the strain in the reinforcement is evaluated, the contribution of the RC slab is quantified through numerical simulations and in addition, the influence of the concrete strength on the failure mechanism is discussed, as well.

## 2. AEM key features

The AEM key features are presented in several papers available in the literature (e.g. [5],[12]). The 3D elements obtained by virtually dividing the structure are assumed to be connected by sets of springs distributed around the edges of each element. Each set of springs comprises one normal and two shear springs, which represent stresses and deformations of the corresponding volume computed from the influence area.

In comparison with Finite Element Method (FEM), in which full compatibility at the nodes is assumed, so that all the neighbouring elements have the same displacement at a node, in AEM the element separation can be easily simulated. This key feature is due to the element face connectivity, so a corner joint of an element may have different displacement compared to the rest. Some springs may fail while others are still effective during analysis so a partial connectivity is easily simulated. Another key feature deriving from connectivity feature is that there is no need for transition elements, which are usually used to switch from large sized elements to smaller ones. Following this feature, the mesh connectivity requirements and interface requirements are brief.

For RC frames, in ELS<sup>®</sup> the springs connecting two adjacent elements may be “matrix springs”, representing the concrete material, and reinforcement springs, denoted “RFT” springs”, representing the existence of steel bars [2]. Three reinforcement springs, one normal and two shear springs, are inserted at the exact location of the steel bars. These springs are removed from the analysis if the reinforcement bar stresses satisfy the steel failure criteria or if the separation strain limit is reached [2].

The concrete in compression is modelled through the Maekawa [2] model. For concrete springs subjected to tension, initial stiffness is assumed until the cracking point, and after cracking the spring stiffness in tension is set to zero. A linear shear stress - shear strain relation is assumed until reaching the cracking point; a drop down of shear stresses depending on aggregate interlock and friction is assumed after the cracking point.

For the reinforcement springs the Ristic et al. [2] model is used, in which the tangent stiffness is calculated based on strain, loading status and loading history of steel spring.

## 3. Experimental investigation

The experiment presented in [1] consists of a third scale planar model of the lower three stories of a multi-story RC frame structure. The model frame characteristics are presented in [1] and are

tabulated in annex A of this paper. Fig. 1 presents the model frame and instrumentation details. A constant vertical force  $F = 109 \text{ kN}$  is acting on top of central column and a step by step unloading process was initiated by lowering the mechanical jacks.

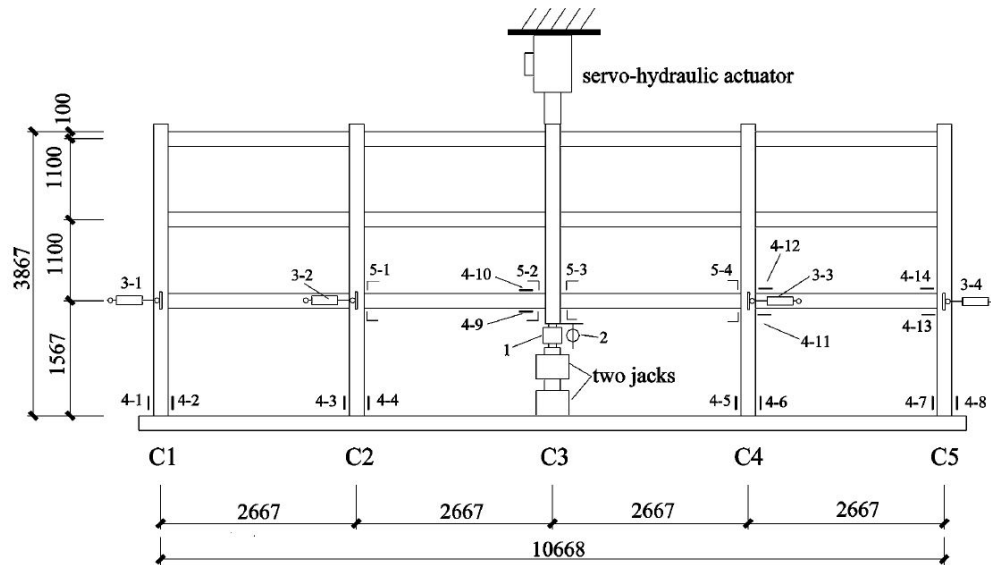


Fig. 1 - Model frame and instrumentation details [1]

#### 4. Comparison of numerical results with experimental results

In the numerical model shown in Fig. 2, the experiment is reproduced by a vertical force  $F = 109 \text{ kN}$  and a static displacement applied on top of the central column. The displacement range is 0-46cm, while the loading is applied in 500 steps. The modelling is done in ELS® software, and the total number of elements is 1274. Both numerical model and the experiment [1], as well as other sources modelling to this experiment [4],[5], describe four deformation stages: Elastic stage A-B corresponding to a vertical displacement less than 5 mm; the elasto-plastic B-C stage in which the vertical displacement is less than 25 mm, the point C in Fig. 3 corresponding to the start of the formation of the plastic hinges; the plastic stage C-D in which plastic rotations of beams ends are registered and severe concrete crushing revealed. Yi et al. [1] notes that after a vertical displacement of 70 mm tension cracks penetrate compression zones. This observation indicates a variation in axial force in beams and this aspect is checked through numerical investigation and shown in Fig.6. The final deformation stage of the experimental frame is the catenary stage D-E, in which the general resisting mechanism changes from compression-bending in beams to tension-bending, as shown in Fig. 7, so in this stage the beams are acting mainly as ties.

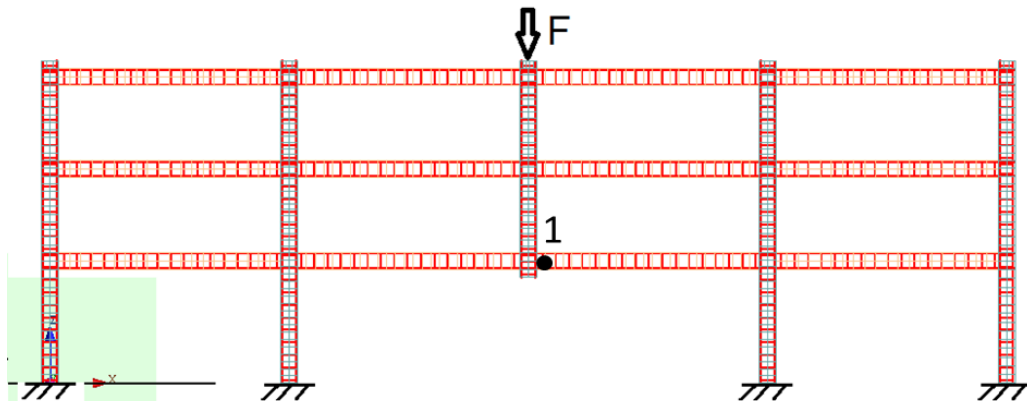
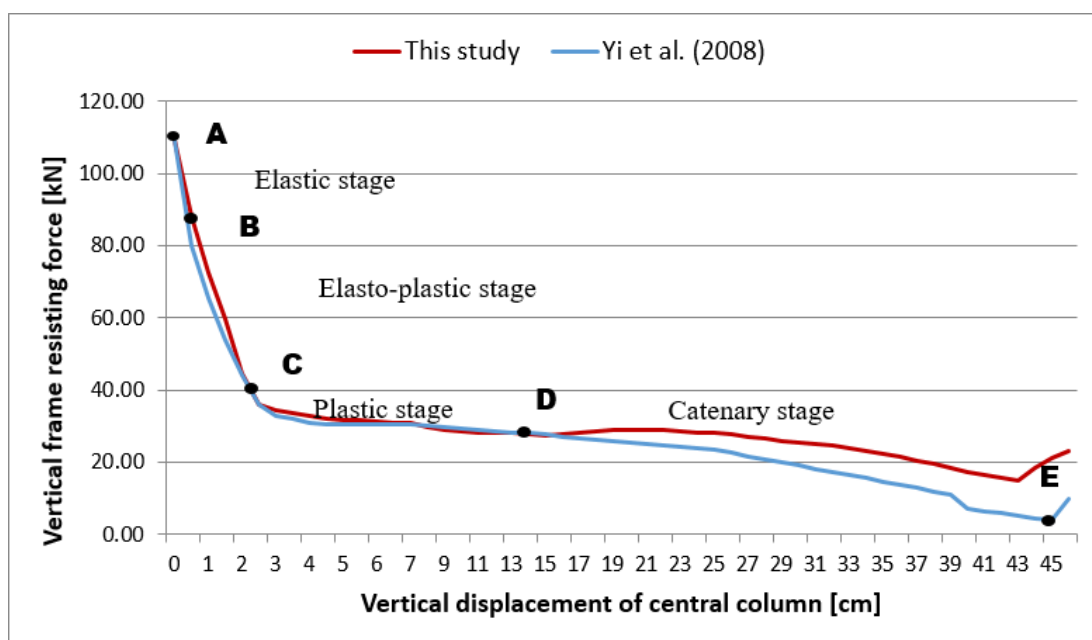
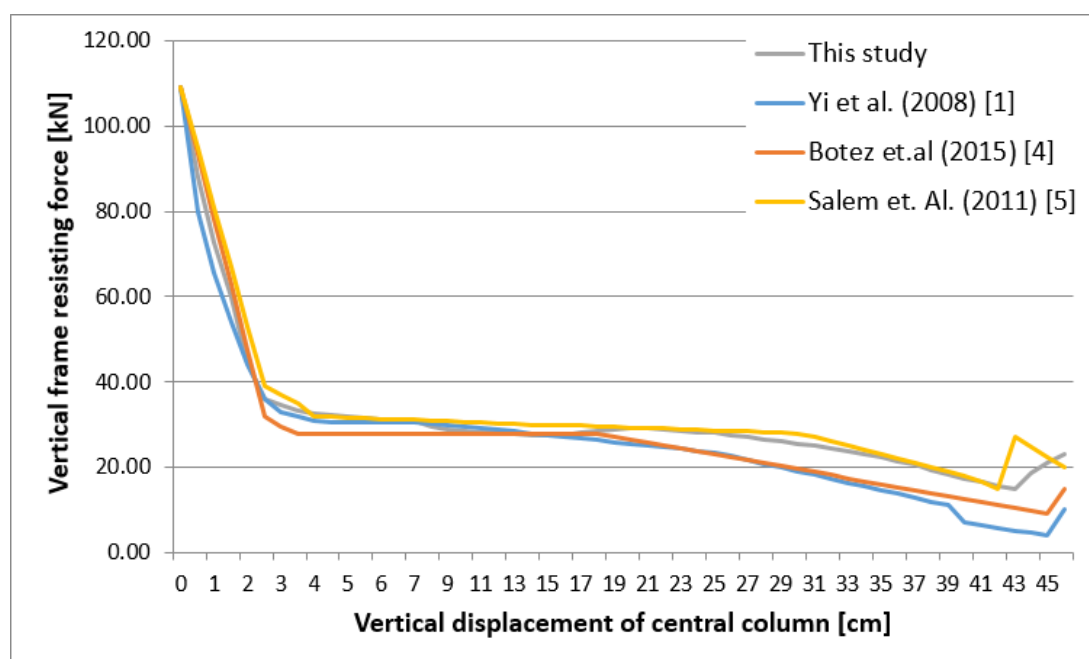


Fig. 2 - Numerical model



**Fig. 3** - Comparison of experimental and numerical results for the resisting vertical force versus vertical displacement

The comparison of some numerical results (vertical resisting force vs. vertical displacement of the central column) obtained in this study with the experimental results and with the results obtained by other researchers is shown in Fig. 4.



**Fig. 4** - Comparison of various results from the literature for the curves showing the resisting force versus vertical displacement

For a better understanding of the frame behaviour during experiment, Fig. 5 presents the variation of the horizontal displacement of sections 3-1 and 3-2 (see Fig. 1) obtained both experimentally [1] and numerically. Thus, Fig. 5 reveals three stages: Stage Ia, in which the adjacent frames are pushed and move outward, stage Ib in which the adjacent frames start being pulled inside, and stage II in which the adjacent frames are pulled inside but the axial force in beams changes in tension.

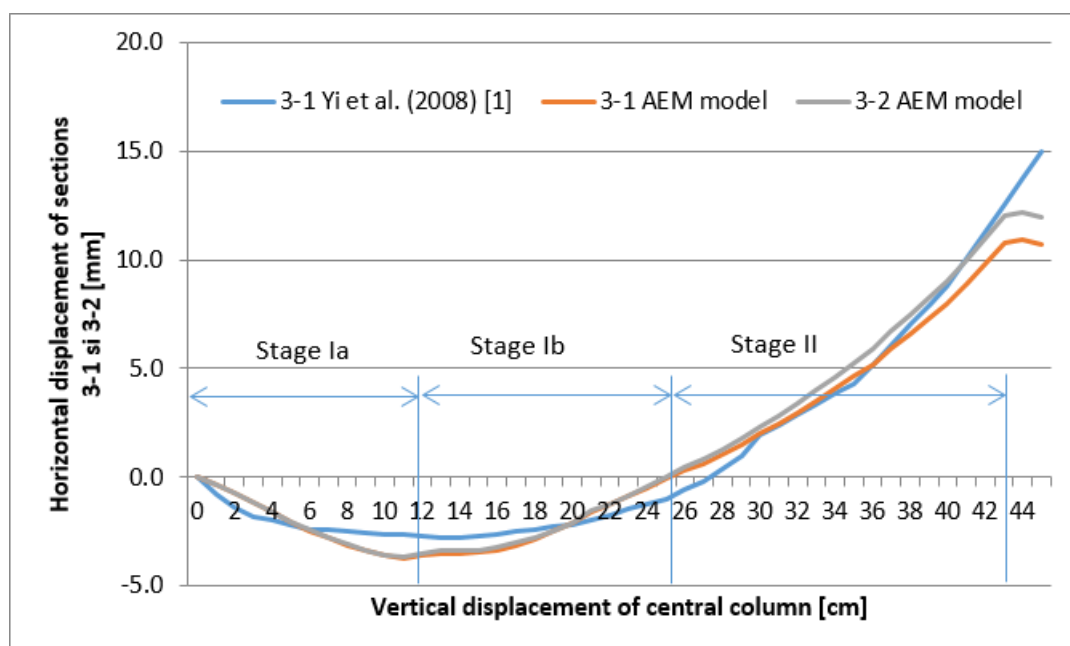


Fig. 5 - Horizontal displacement in sections 3-1 and 3-2 versus vertical displacement of central column, obtained experimentally [1] and numerically.

Fig. 6 presents the variation of the axial force in cross-section 1 as denoted in Fig. 2. In stage Ia the stress resultant in the beam is a compression force that pushes the adjacent frames outwards, while the tension stress resultant in reinforcing bars leads to elongation and consequently to yielding. A drop in the axial force is recorded at a vertical displacement of around 125 mm suggesting that the adjacent frames start moving towards inside, which is consistent to stage Ib. In stage II, the vertical displacement is large enough so as the compressed diagonal do not exist anymore, and the beams behave mostly in tension, as ties. Fig. 7 presents the variation of the axial force with respect to the bending moment measured in cross-section 1.

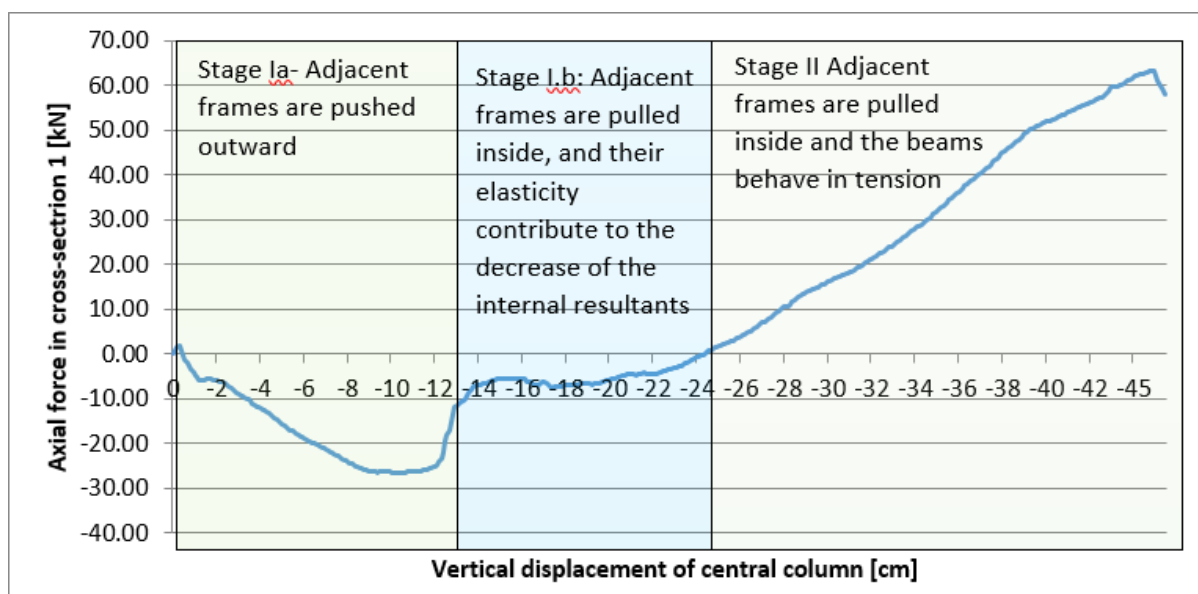


Fig. 6 - Axial force variation with respect to vertical displacement of central column

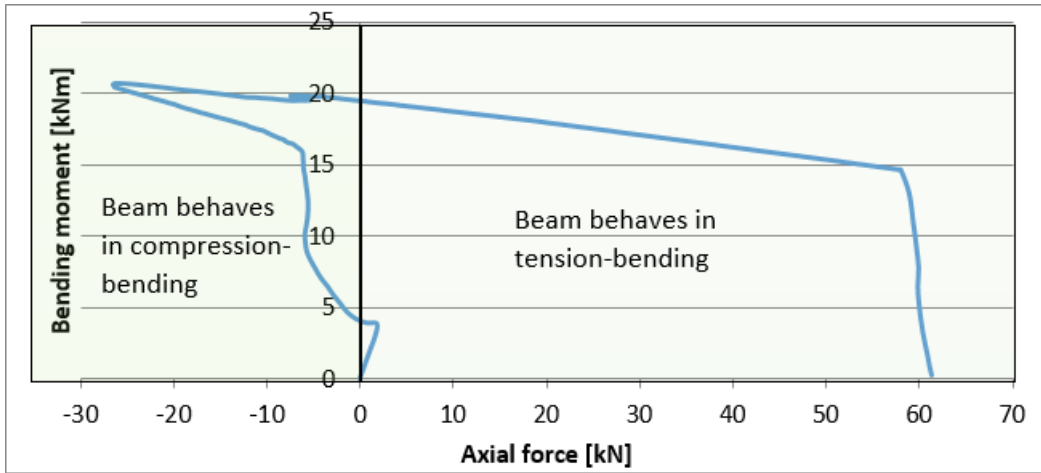


Fig. 7 - Axial force (horizontal, [kN]) versus bending moment (vertical, [kNm]) measured in cross-section 1

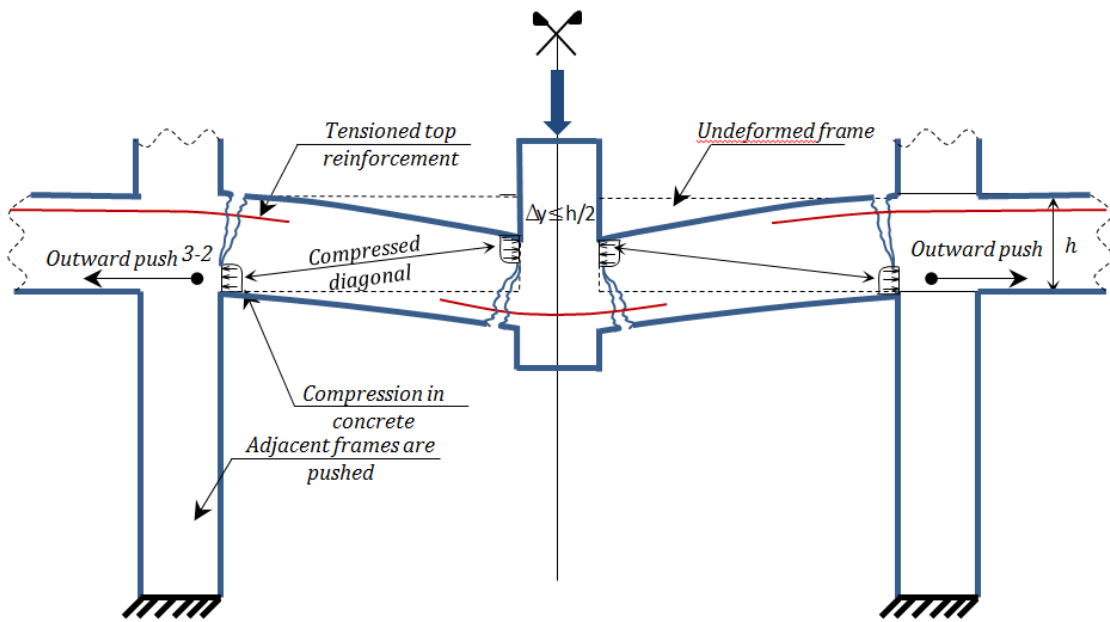


Fig. 8 - Stage Ia – Adjacent frames are pushed outward

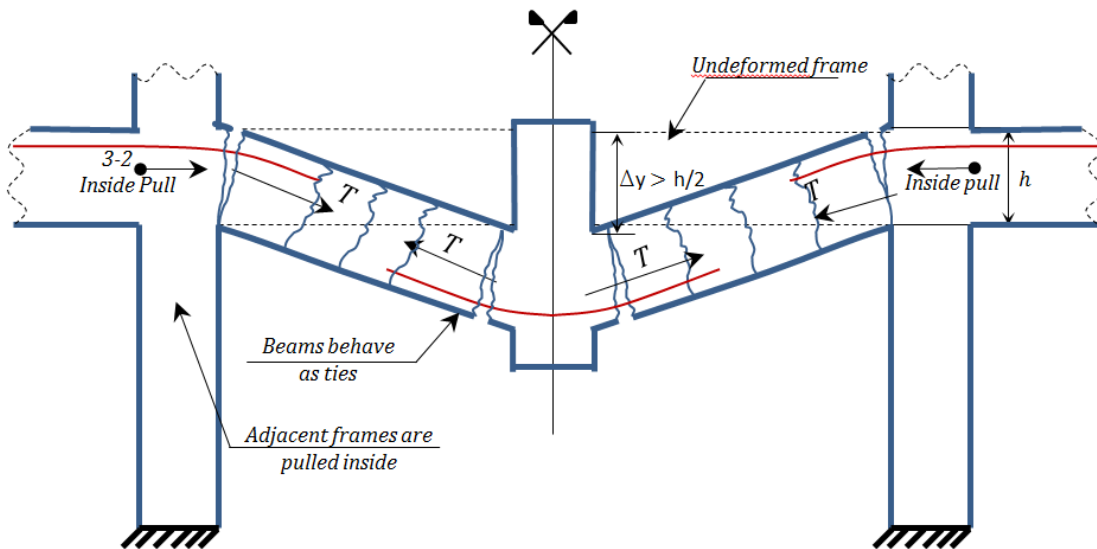


Fig. 9 - Stage II – Adjacent frames are pulled inside and beams behave as ties.

Each level of the adjacent frames deforms under vertical loading of central column. Fig 10 and 11 present the lateral displacement of sections 3-1 located at each floor with respect to the vertical displacement of the central column. The maximum lateral displacements of sections 3-1 increase with height, from 11,9 mm to 21,3 mm at the top floor.

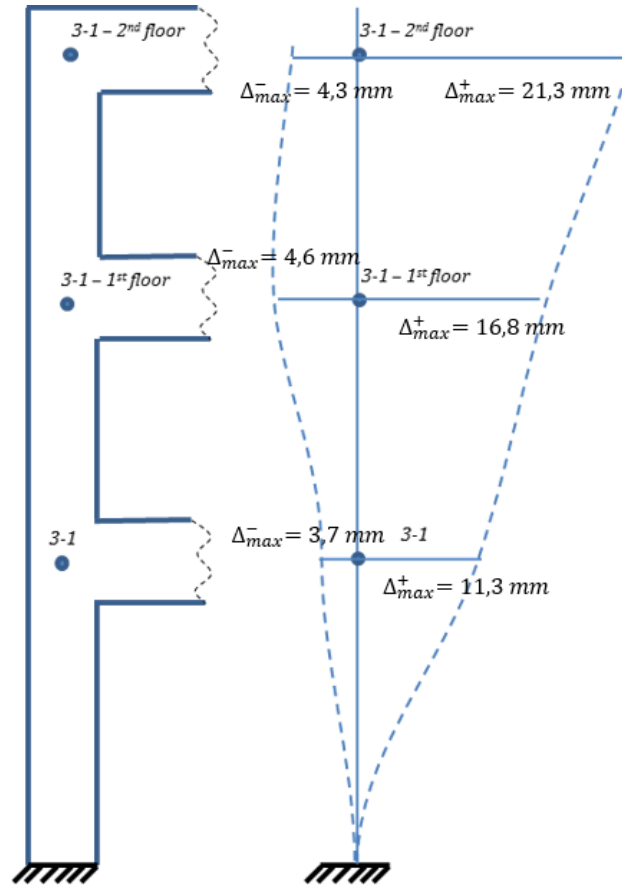


Fig. 10 - Extreme values of lateral displacements of sections 3-1 located on the marginal column at each story level.

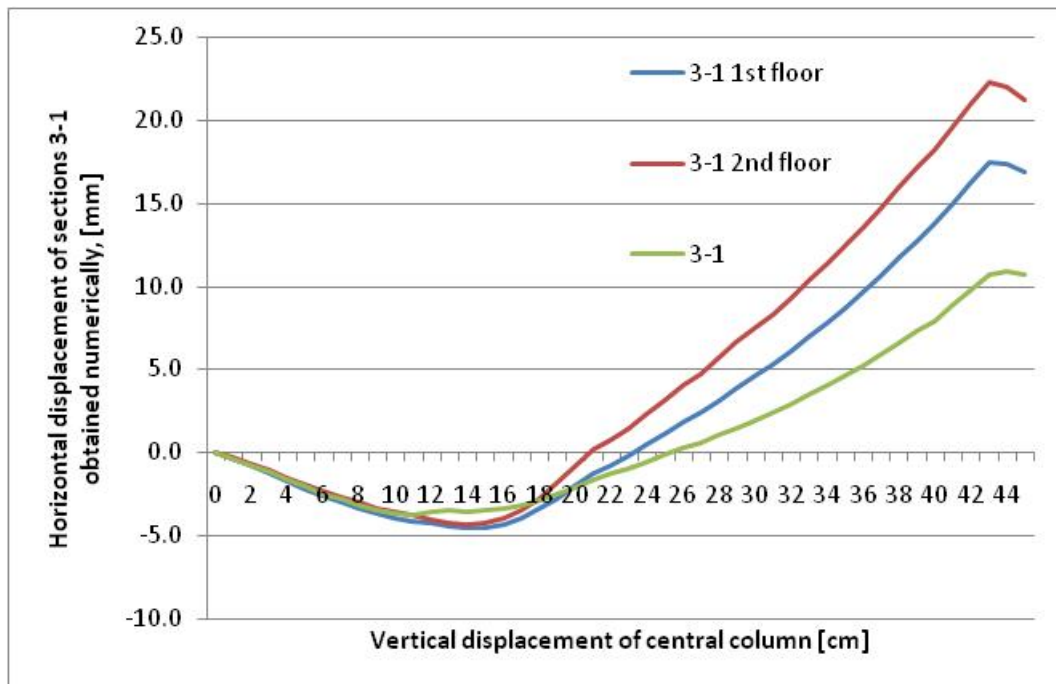


Fig. 11 - Horizontal displacement of sections 3-1 located at each story – vertical displacement of central column

The good match between the numerical results obtained in this study and the experimental ones suggest that further numerical investigation can be performed. The initial work [1] states that the model frame is a part of multi-story frame structure, in which the existence of the slab limits the relative lateral displacements of columns. A limit case can be considered if the relative lateral displacements of columns are set to zero. Furthermore, the contribution of the slab is evaluated not through its own mass and stiffness, but through its indirect effect of limiting the relative lateral displacement of the columns.

## 5. Evaluation of the indirect contribution of slab

A new numerical model is derived based on the one previously shown, in which sections 3-1 and 3-4 located at the extremities of beams of each floor have zero horizontal displacements, as depicted in Fig. 12.

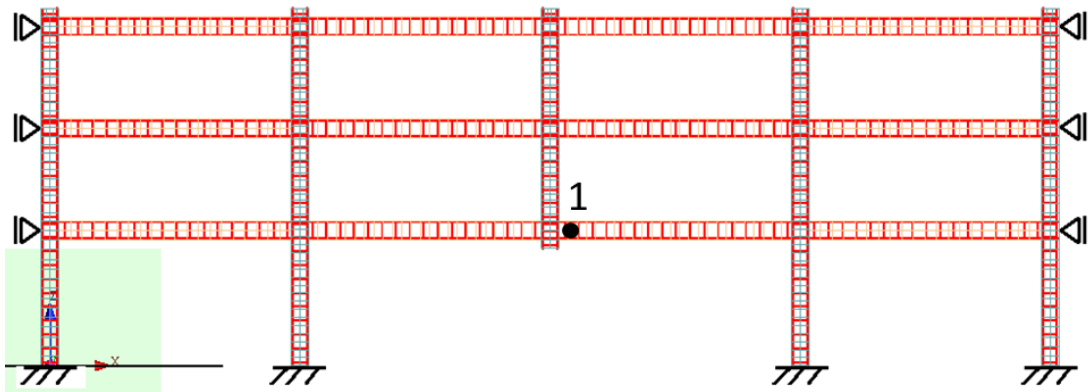
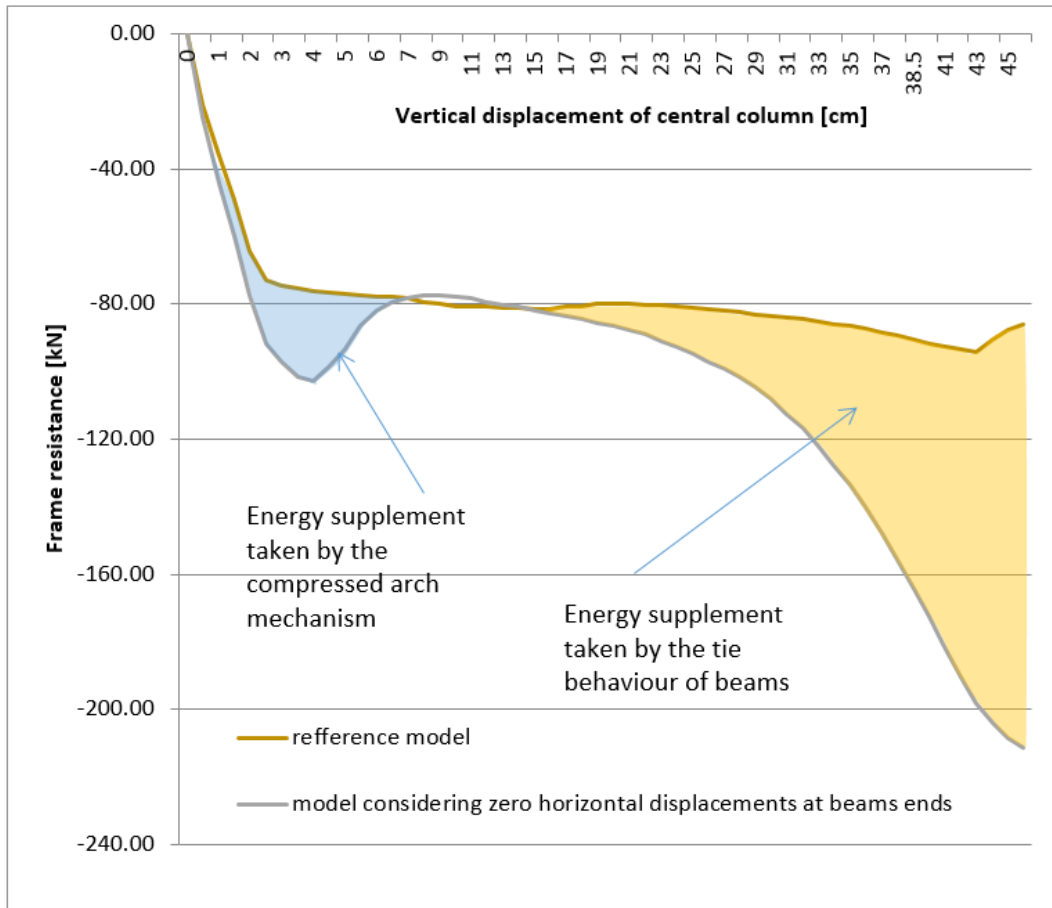


Fig. 12 - Numerical model which considers zero horizontal displacement for sections 3-1 and 3-4.

For a better comparison between the two models, we analyse only the case when the imposed vertical displacement is applied. In this manner the variation depicted in Fig. 3 is shifted by 109 kN towards the horizontal axis, as shown in Fig. 13. The energy induced in the system is the work done by the imposed displacement, the work being transformed into strain energy. In this way, one can compute the necessary energy needed to obtain the fracture of the first longitudinal bars as the area below the force-displacement graph.

Introducing a set of restraints will lead to a superior stiffness as compared to the initial (reference) numerical model. It is expected that the energy induced in the system necessary to obtain the same vertical displacement as in the reference model is superior to that of the reference model. However, it is interesting to note which resisting mechanism will support the supplementary energy. Another question that arises is if the bottom bars will still fracture, and if so, at which vertical displacement. The resistance of the frame versus vertical displacement in both numerical models is shown in Fig. 13. Because the outward displacement of adjacent frames is no longer allowed, a supplementary energy is taken by the compressed beams. The resistance of the frame is almost equal in both numerical models in the range 60 mm-150 mm vertical displacement of the central column. In the catenary stage, because the inside pulling of adjacent frames is no longer permitted, a supplementary energy is taken by the beams through a tie behaviour. The energy below the frame resistance – vertical displacement in the reference model model is  $L_{ext} = 36,91kJ$ , while the same energy in the model considering zero horizontal displacement for beams is  $L_{ext} = 49,66kJ$ . Thus, a difference of 12,75kJ, which represents 35% over-strength of the second model, is obtained. The supplementary energy is taken by the compressed arch behaviour of the beams (0,8kJ, which represents 6% of the supplementary energy) and by the tie behaviour of beams (12,3kJ, which represents 95% of the supplementary energy). Less than 1% of the energy difference is calculated in the range 60..150 mm vertical displacement, so the authors consider the same resistance force of the frame in this range.

Neglecting the compressed arch behavioursupplementary energy, which represents less than 2% of the total energy, it can be stated that both models have the same overall behaviour in the range 0..150mm vertical displacement, the major difference being the capacity of the beams with tie behaviour. This behaviour is due to the fact that both top and bottom reinforcing bars contribute to the tie mechanism, and a more even strain distribution between these bars is observed. The variation of the strain in the reinforcing bars is depicted in Fig. 17 and Fig. 18.



**Fig. 13** - Comparison between the reference model and the model that considers zero horizontal displacement at the beam ends

Fig 14 a),b) depict the variation of the axial force and bending moment respectively, measured in cross-section 1 denoted in Fig. 12 with respect to the vertical displacement of the central column. Fig. 15 displays the variation of the axial force with respect to bending moment measured in cross-section 1; the change in the resisting mechanism type can be seen, from compression-bending to tension-bending.

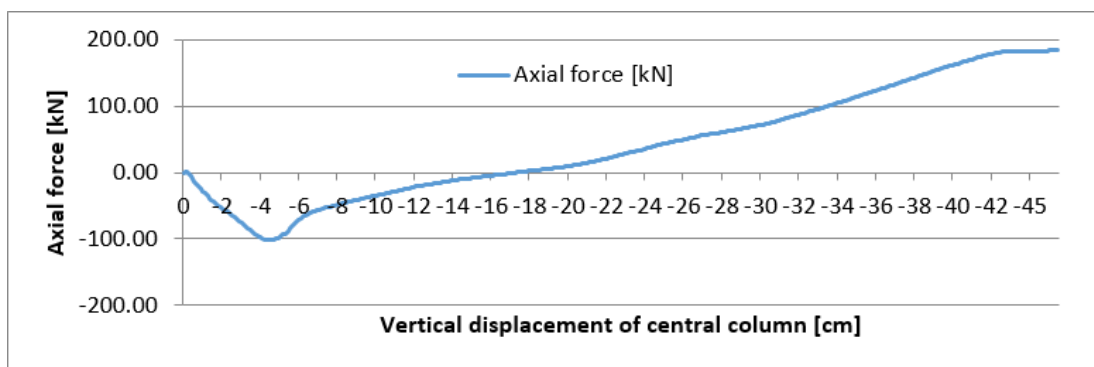


**Fig. 14** - a) Variation of the axial force measured in cross-section 1 with respect to vertical displacement of central column

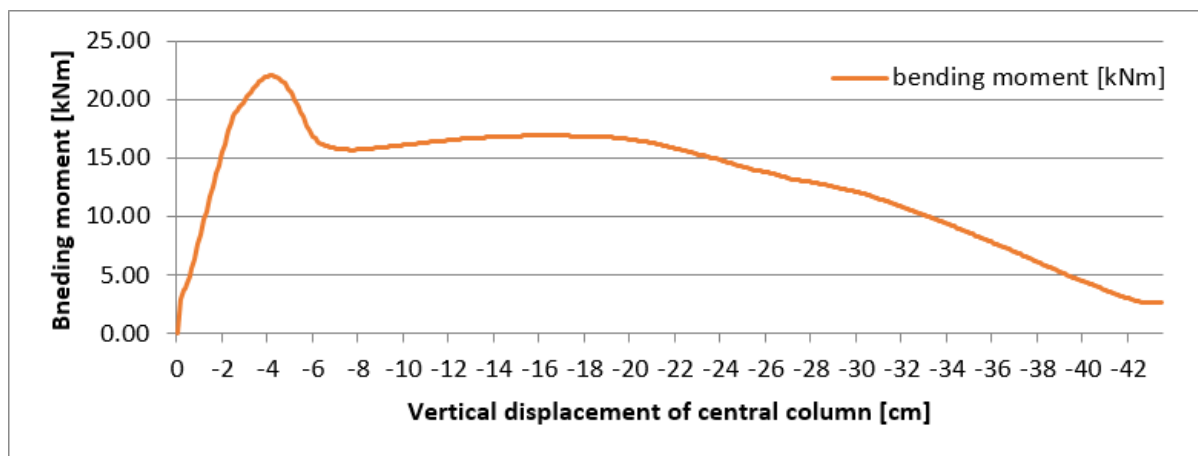


Fig. 14 - b) Variation of the bending moment measured in cross-section 1 with respect to vertical displacement of central column

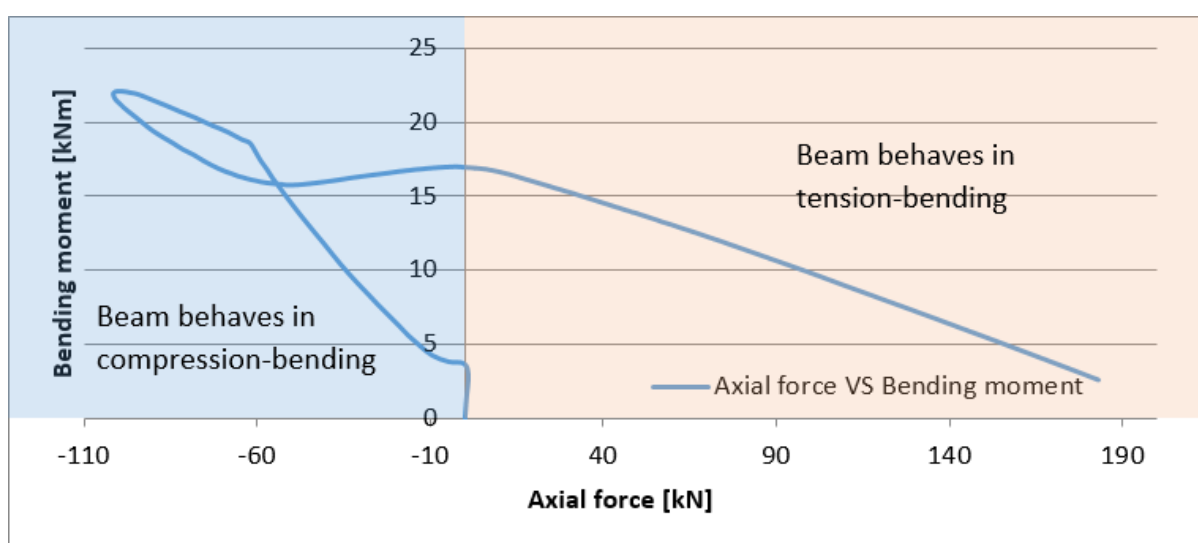


Fig. 15. Axial force versus bending moment in cross-section 1

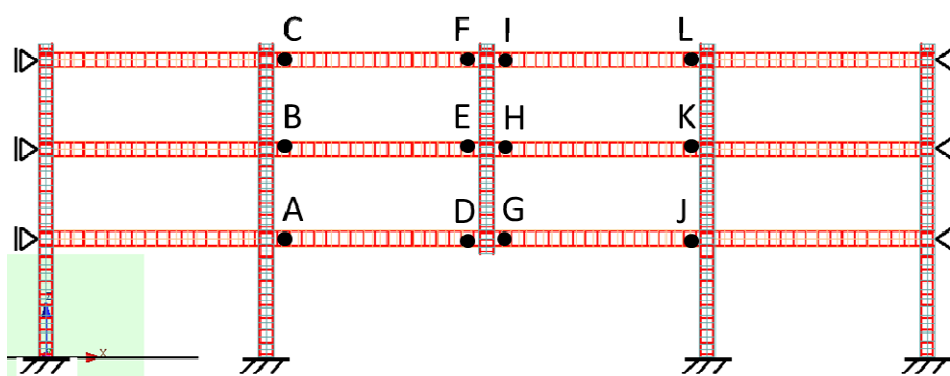
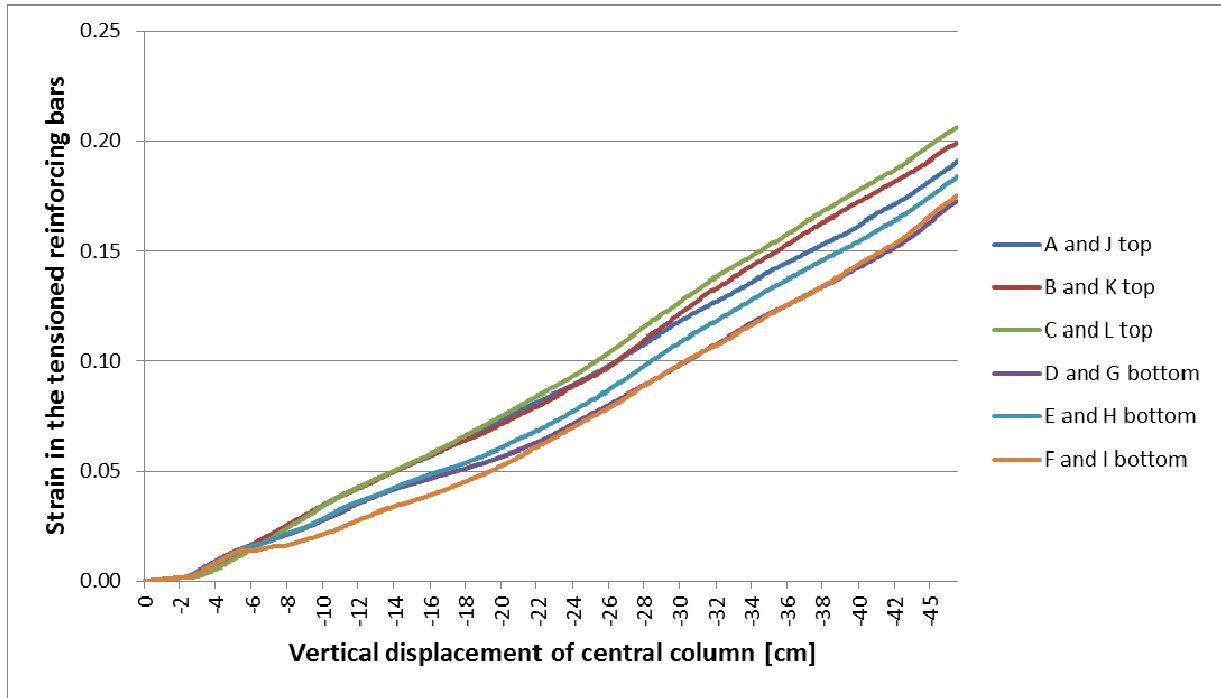
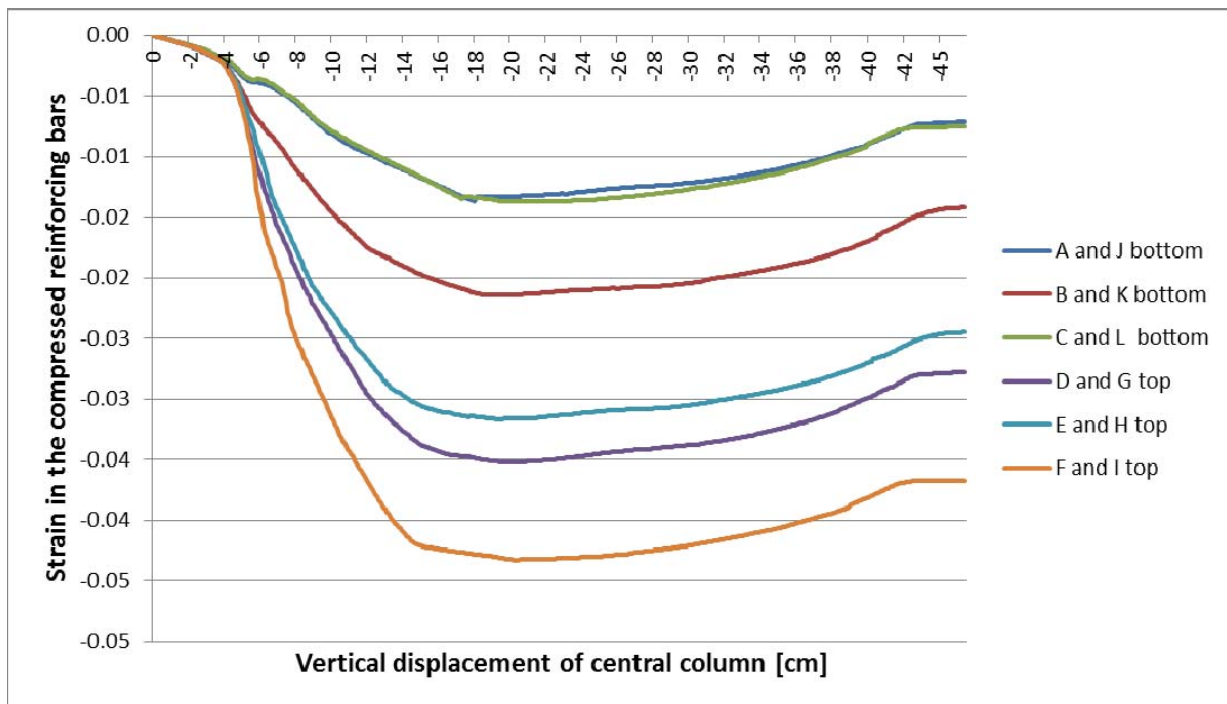


Fig. 16 - Positions of the sections in which the strain in the reinforcing bars is monitored.

Fig. 16 presents the cross-sections where the strain in the reinforcing bars is monitored. Fig. 17 presents the variation of the strain in the tensioned reinforcing bars; the ultimate strain being 0.22, less than 0.275 specified in the material data given in [1], which means that no reinforcing bars fracture occurs. In addition, Fig. 18 presents the variation of the strain in the compressed reinforcing bars, where a decrease in the strain occurs at around 140 mm vertical displacement of the central column.



**Fig. 17** - Strain in the tensioned reinforcing bars vs. vertical displacement of central column



**Fig. 18** - Strain in the compressed reinforcing bars vs vertical displacement of central column

## 6. Influence of concrete strength on the failure mechanism

The reference frame discussed in Chap. 4 is further investigated. The influence of concrete strength on the failure mechanism is modelled in two additional cases through a lower concrete compressive strength of 15MPa and a higher compressive strength of 35MPa. The results are compared (with the reference failure mechanism presented in Fig.3) in Fig. 19. Fig. 19 shows that by decreasing the concrete strength from 25MPa to 15MPa, the first fracture of the reinforcing bars appears at 45cm instead of 43cm vertical displacement in the reference frame.

Increasing the concrete strength induces early fracture of the reinforcing bars at around 30cm vertical displacement. The fracture of the bars decreases the overall resistance of the frame.

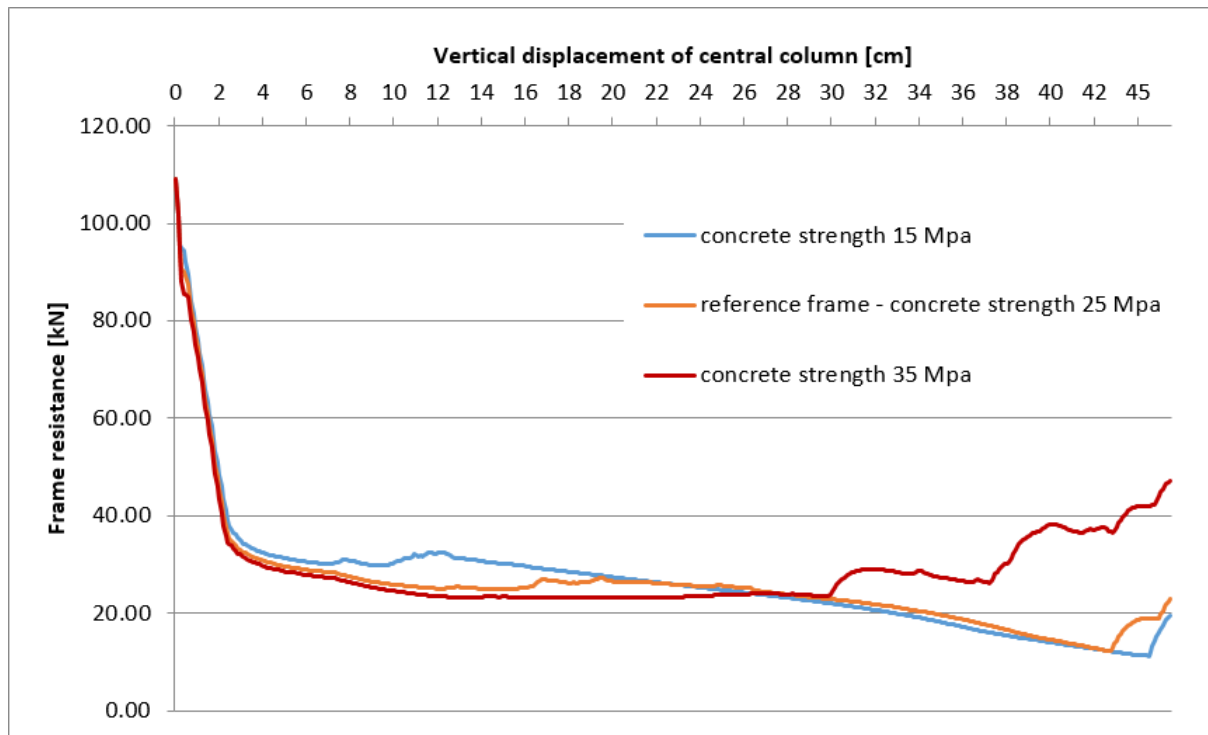


Fig. 19 - Evaluation of the influence of the concrete strength on the RC frame resistance

## 7. Conclusions

In this study, a numerical investigation is conducted based on experimental data. The experiment consists of a third scale planar model of the lower three stories of a multi-story RC frame structure. The numerical investigation is conducted through the use of a dedicated software (Extreme Loading® for Structures) which is based on the Applied Element Method (AEM). The main findings in this study can be summarized as follows:

- Very good match between the experimental and numerical data has been obtained. Thus, four deformation stages are observed: an elastic stage A-B followed by an elasto-plastic B-C. Subsequently, a plastic stage C-D occurs and finally the catenary stage D-E which leads to the failure of the model RC frame.
- The variation of the horizontal displacement for two sections reveals three-stage mechanism related to the behavior of the model RC frame. The adjacent frames with respect to the loading point are firstly pushed towards the exterior and much later (for vertical displacements of the loaded column in excess of 25 mm) are pulled towards the interior, as depicted in Fig. 11.
- 95% of the supplementary energy induced by restraining the horizontal displacements of the columns is taken through the tie behavior of the beams.
- No fracture of the tensioned reinforcement is observed from the investigation considering restrained horizontal displacements.
- Through the increase of the concrete strength an early fracture of the reinforcing bars at around 30 cm vertical displacement is induced. Consequently, the fracture of the bars will eventually lead to the decrease of the overall resistance of the frame.

## ANNEX A – Planar RC frame characteristics taken from [1]

Table A1

Dimensions of 1/3 model frame

Structure characteristics		Prototype frame [m]	1/3 Model frame [m]
Floor Height	Ground floor	4,70	1,567
	1 <sup>st</sup> and 2 <sup>nd</sup> floors	3,30	1,10
Bay span		8,00	2,667
Beams ( depth x width )		0,6 x 0,3	0,2 x 0,1
Columns ( depth x width )		0,6 x 0,6	0,2 x 0,2
Axial force on top of central columns		981kN	109kN

TabelA2

Dimensions and reinforcing details of 1/3 model frame

Element	Dimensions [cm]	Longitudinal reinforcement		Transversal reinforcement
Beam	10x20	Top bars 2 $\phi$ 12	Bottom bars 2 $\phi$ 12	$\Phi$ 6/15cm
Column	20x20	4 $\phi$ 12		$\Phi$ 6/15cm

$\phi$ 12 bars have nominal diameter of 12mm.

TabelA3

Reinforcing steel and concrete properties

Material	Item	Measured values
Longitudinal reinforcement (HRB 400)	Yield strength [Mpa]	416
	Ultimate tensile strength [Mpa]	526
	Ratio of elongation	27.5%
Transversal reinforcement (HPB235)	Yield strength [Mpa]	370
	Concrete C30	Cubic strength* [Mpa]

\* Cubic strength is measured with respect to cube having 150mm edges.

## Acknowledgements

The authors thank to the Applied Science International company for providing an educational licence of the ELS® software.

## References

- [1] Yi WJ, He QF, Xiao Y, Kunnath, SK. (2008). Experimental study on progressive collapse-resistant behaviour of reinforced concrete frame structures. *ACI Struct J*, 105(4):433-439.
- [2] Extreme Loading® for Structures Theoretical Manual (2013). Applied Science International.
- [3] Meguro K, Tagel-Din H. ((2010). Applied element method for structural analysis: theory and application for linear materials. *StructEng/EarthqEng JSCE*; 17:21s-35s.
- [4] Botez M, Bredean L, Ioani A. (2016). Improving the accuracy of progressive collapse risk assessment: Efficiency and contribution of supplementary progressive collapse resisting mechanisms. *ComputStruct*; DOI: 10.1016/j.compstruc.2015.11.002.
- [5] Salem HM, El-Fouly AK, Tagel-Din HS. (2011) Toward an economic design of reinforced concrete structures against progressive collapse. *EngStruct*, 33:3341-3350.

- [6] Li Y, Lu X, Guan H, Ye L. (2011). An improved tie force method for progressive collapse resistance design of reinforced concrete frame structures. *EngStruct*, 33:2931-2942.
- [7] Shan S, Li S, Xu S, Xie L. (2016). Experimental study on the progressive collapse performance of RCframes with infill walls. *EngStruct*, 111:80-92.
- [8] Brunesi E, Nascimbene R, Parisi F, Augenti N. (2015). Progressive collapse fragility of reinforced concrete framed structures through incremental dynamic analysis. *EngStruct* 104:65-79.
- [9] Kazemi-Moghaddam A, Sasani M. (2015). Progressive collapse evaluation of Murrah Federal Building following sudden loss of column G20. *EngStruct*, 89:162-171.
- [10] Kokot S, Anthoine A, Negro P, Solomos G. (2012). Static and dynamic analysis of a reinforced concrete flat slab frame building for progressive collapse. *EngStruct*, 40:205-217.
- [11] Wang H, Su Y, Zeng Q. (2011). Design methods of reinforced-concrete frame structure to resist progressive collapse in civil engineering. *Sys EngProc*; 1:48-54.
- [12] Salem HM, Helmy HM. (2014). Numeircal investigation of collapse of the Minnesota I-35W bridge. *EngStruct* 2014; 59:635-645.